Mass-redistributed method in the evaluation of eigenfrequency of solid systems

Eric Li^{1,2*}, ZC He¹, Xu Xu²

¹State Key Laboratory of Advanced Design and Manufacturing for Vehicle Body, Hunan University, Changsha, 410082 P. R. China

¹2College of Mathematics, Jilin University, Changchun 130012, China

Abstract

Due to overly-stiff effect, standard Finite Element Method (FEM) using triangular and tetrahedral elements gives upper bound solution of natural frequencies. In order to improve the simulation results using low-order elements, one approach is to soften the overly-stiff of stiffness matrix to simulate the exact system, and the other is to match the mass matrix to the overly-stiff system. In this paper, the mass-redistributed method is further extended to analyse the eigenfrequency of solid systems. The mass-redistributed method is to modify the mass matrix of the discrete systems by shifting the integration points away from the Gaussian locations, while ensuring the mass conservation. Numerical examples including 2D and 3D problems have verified that Gaussian integration point in the mass matrix has a significant effect in the evaluation of eigenfrequency.

key words: Mass-redistributed Method; Finite Element Method; Eigenfrequency

1. Introduction

The overly-stiff finite element method predicts upper bound solution of eigenfrequency [1]. In order to soften the overly-stiff effect, smoothed finite element method (SFEM) is developed [2]. With different types of smoothing domain, edge-based smoothed finite element method (ES-FEM) [3-9], node-based smoothed finite element method (NS-FEM) [10], alpha finite element method (α FEM) [11-13] and hybrid smoothed finite element method (HS-FEM) [14-17] have been formulated and applied to heat transfer, biomechanics, acoustic problems. The SFEM with right softened effect is able to achieve a close to exact stiffness, which provides more accurate solution of eigenfrequencies compared with finite element method.

Alternatively, the balance of discrete model between mass and stiffness can be achieved with modification of mass matrix. For example, a weighted average of the consistent and lumped mass matrices has been proposed by Marfurt in the computation of the mass matrix for acoustic and elastic wave propagation problems [18]. In addition, a new modified integration rules in the calculation of the mass and stiffness for acoustic problems for quadrilateral mesh is developed by Murthy [19]. He et al have further proposed mass-redistributed method to reduce the dispersion error in acoustic problems [20]. The redistribution of mass matrix of the discrete systems will be modified by shifting the integration points away from the usual Gaussian locations [20]. In this paper, we further extend mass-redistributed method in the analysis of eigenfrequency.

The paper is organized as follows: Section 2 briefly describes the formulation of mass-redistributed method in the computation of eigenfrequency. Numerical examples including 2D and 3D are presented in Section 3 to investigate the effect of Gaussian integration point on eigenfrequency using mass-redistributed method. Finally the conclusions from the numerical results are made in Section 4.

Email address: ericsg2012@gmail.com

1

^{1*}Corresponding author.

2. Materials and Methods

2.1. 2D Mass-redistributed method

The standard FEM behaves stiffer than the exact system, which causes larger eigenvalues compared to exact one.

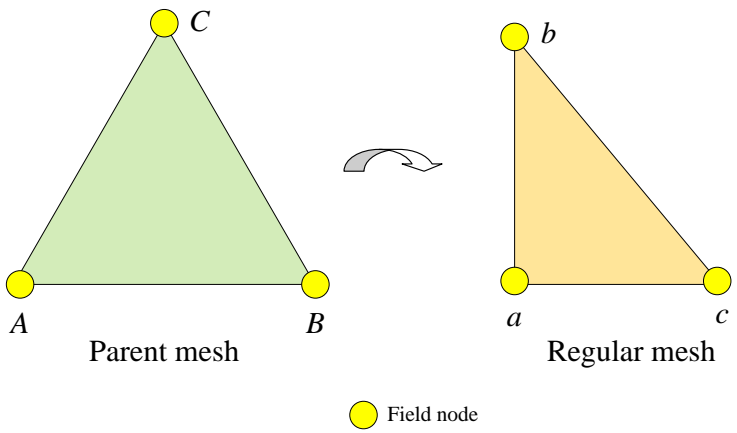


Figure 1: Transformation of triangular mesh

In the formulation of 2D mass-redistributed method, the first step is to transform parent mesh to regular mesh as shown in Fig. 1 [20]. Hence, the integration of stiffness and mass matrix is transformed into the natural coordinate system as follows:

$$\mathbf{K}^{e} = \int_{-1}^{+1} \int_{-1}^{+1} (\nabla \mathbf{N})^{T} (\nabla \mathbf{N}) \det(J) d\xi d\eta, \quad \mathbf{M}^{e} = \int_{-1}^{+1} \int_{-1}^{+1} \mathbf{N}^{T} \mathbf{N} \det(J) d\xi d\eta, \quad (1)$$

At the same time, the linearly shape function $N_i(x)$ can be written in the area coordinates form as shown in Fig. 2.

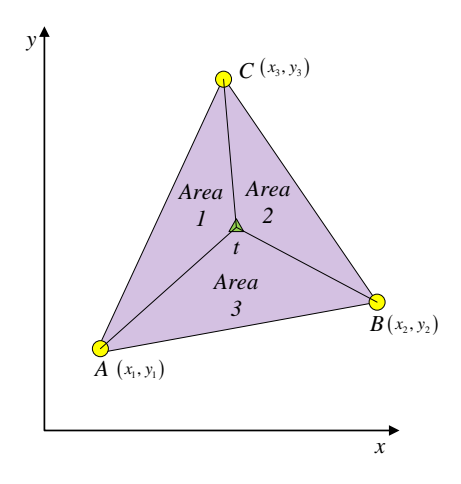


Figure 2: Area coordinates for a linear triangular element

With connection t to three vertices 1, 2, 3, three sub-areas A_1 , A_2 , and A_3 corresponding to the triangles tAC, tBC and tBA, respectively can be determined for any given point t within the element. Using area coordinates, the shape functions for each node are expressed as follows:

$$N_1 = \frac{A_1}{A} = 1 - \xi - \eta \; ; \; N_2 = \frac{A_2}{A} = \xi \; ; \; N_3 = \frac{A_3}{A} = \eta$$
 (2)

With Gauss quadrature rule, Eq. (1) can be evaluated:

$$\int_{-1}^{+1} \int_{-1}^{+1} \phi d\xi d\eta = \sum_{i=1}^{ng} w_i \phi(\xi_i, \eta_i)$$
 (3)

where ng is the number of Gauss points, w_i are the weights and ξ , η are the local coordinates of Gauss points. Then the generalized stiffness and mass matrix can be obtained by the integration rule.

$$\mathbf{K}^{e} = w_{i} \left(\nabla \mathbf{N} \left(\xi_{i}, \eta_{i} \right) \right)^{T} \left(\nabla \mathbf{N} \left(\xi_{i}, \eta_{i} \right) \right) \det(J)$$

$$\mathbf{M}^{e} = \sum_{i=1}^{3} w_{i}^{k} \left(\mathbf{N} \left(\xi_{i}^{k}, \eta_{i}^{k} \right) \right)^{T} \left(\mathbf{N} \left(\xi_{i}^{k}, \eta_{i}^{k} \right) \right) \det(J)$$
(4)

From Eq. (4), we can notice that the gradient of shape function using triangular mesh is constant within the elements and thus the integration of stiffness matrix in Eq.(4) equals to the constant multiplied by the Jacobi.

The consistent mass matrix is evaluated by three Gauss points with $w_i = 1/3$.

point 1:
$$\xi_i = 2/3$$
, $\eta_i = 1/6$ point 2: $\xi_i = 1/6$, $\eta_i = 2/3$ point 3: $\xi_i = 1/6$, $\eta_i = 1/6$ (5)

On the other hand, the lumped mass matrix is formed with the following points:

point 1:
$$\xi_i = 1$$
, $\eta_i = 0$ point 2: $\xi_i = 1/6$, $\eta_i = 2/3$ point 3: $\xi_i = 1/6$, $\eta_i = 1/6$ (6)

The generalized mass matrix is evaluated by introducing a variable integration point t:

$$\xi_{i} = t, \quad \eta_{i} = \frac{1-t}{2} (\text{Point 1}),$$

$$\xi_{i} = \frac{1-t}{2}, \quad \eta_{i} = t (\text{Point 2})$$

$$\xi_{i} = \frac{1-t}{2}, \quad \eta_{i} = \frac{1-t}{2} (\text{Point 3})$$
(7)

where $t \in [0,1]$, and weight $w_i = 1/3$ so that $\sum_{i=1}^{3} w_i = 1$.

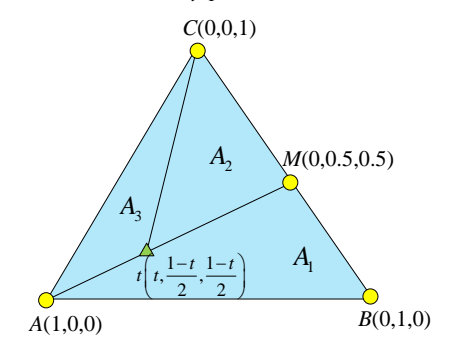


Figure 3: Modified integration point for the mass matrix of linear triangular element

It is noticed that the integration point will move from a triangular vertex to midpoint of the edge opposite to the vertex, as shown in Fig. 3 as *t* varies from 0 to 1.

Using these three sampling points, the mass matrix can be expressed in terms of parameter

t as:

$$\mathbf{M}^{e} = \frac{1}{3} A^{e} \begin{bmatrix} a_{11} & 0 & a_{13} & 0 & a_{15} & 0 \\ 0 & a_{22} & 0 & a_{24} & 0 & a_{26} \\ a_{31} & 0 & a_{33} & 0 & a_{35} & 0 \\ 0 & a_{42} & 0 & a_{44} & 0 & a_{46} \\ a_{51} & 0 & a_{53} & 0 & a_{55} & 0 \\ 0 & a_{62} & 0 & a_{64} & 0 & a_{66} \end{bmatrix}$$
(8)

where

$$a_{11} = a_{22} = a_{33} = a_{44} = a_{55} = a_{66} = t^2 + \frac{(1-t)^2}{2}$$

$$a_{13} = a_{15} = a_{24} = a_{26} = a_{31} = a_{35} = a_{42} = a_{46} = a_{51} = a_{53} = a_{62} = a_{64} = t(1-t) + \frac{(1-t)^2}{4}$$

The summation of all matrix elements of \mathbf{M}^{e} equals to the area of the element regardless of value of t:

$$\sum_{i=1}^{36} \frac{1}{6} A^e \mathbf{M}_i^e = A^e$$
total area of the element (9)

The eigenvalues are determined by the stiffness and mass matrix:

$$\omega^{2} I = \frac{\boldsymbol{\phi}^{T} \mathbf{K} \, \boldsymbol{\phi}}{\boldsymbol{\phi}^{T} \mathbf{M} \, \boldsymbol{\phi}} = \begin{bmatrix} \frac{\lambda_{k1}}{\lambda_{m1}} & & & \\ & \frac{\lambda_{k2}}{\lambda_{m2}} & & \\ & & \ddots & \\ & & & \frac{\lambda_{kn}}{\lambda_{mn}} \end{bmatrix}$$
(10)

where $\lambda_{k_1} \sim \lambda_{k_n}$ are the eigenvalues of stiffness matrix **K**, $\lambda_{m_1} \sim \lambda_{m_n}$ are the eigenvalues of mass matrix.

2.2. 3D Mass-redistributed method

In the formulation of 3D mass-distributed method using linear tetrahedral element, the mapping from a parent tetrahedral mesh to the regular tetrahedral mesh is based on volume coordinates. Thereby, the integration of stiffness and mass matrix is transformed into the natural coordinate system as follows:

$$\mathbf{K}^{e} = \int_{-1}^{+1} \int_{-1}^{+1} \int_{-1}^{+1} \int (\nabla \mathbf{N})^{T} (\nabla \mathbf{N}) \det(J) d\xi d\eta d\zeta,$$

$$\mathbf{M}^{e} = \int_{-1}^{+1} \int_{-1}^{+1} \int_{-1}^{+1} \mathbf{N}^{T} \mathbf{N} \det(J) d\xi d\eta d\zeta,$$
(11)

Similarly, the linearly shape functions is expressed in the volume coordinates form as shown in Fig. 4.

Four sub-volumes V_1 , V_2 , V_3 and V_4 corresponding to the tetrahedron tBCD, tACD, tABD and tABC, respectively can be determined for any given point t within the element. Hence, the

shape function is formulated as follows:

$$N_{1} = \frac{V_{tBCD}}{V_{ABCD}} = 1 - \xi - \eta - \zeta \; ; \quad N_{2} = \frac{V_{tACD}}{V_{ABCD}} = \xi \; ;$$

$$N_{3} = \frac{V_{tABD}}{V_{ABCD}} = \eta \; ; \qquad N_{4} = \frac{V_{tABC}}{V_{ABCD}} = \zeta$$

$$A \qquad \qquad B \qquad \qquad a \qquad \text{Regular mesh}$$
(12)

Figure 4: Volume coordinate using tetrahedral mesh

Similar to 2D case, the Gaussian integration point t controls the formulation of 3D mass matrix. For example, the consistence mass matrix is evaluated by using following four Gauss points with weight $w_i = 1/4$:

point 1:
$$\xi_i = 0.5854102$$
, $\eta_i = 0.1381966$, $\zeta_i = 0.1381966$, point 2: $\xi_i = 0.1381966$, $\eta_i = 0.5854102$, $\zeta_i = 0.1381966$ point 3: $\xi_i = 0.1381966$, $\eta_i = 0.1381966$, $\zeta_i = 0.5854102$ point 4: $\xi_i = 0.1381966$, $\eta_i = 0.1381966$, $\zeta_i = 0.1381966$

Using the following four Gauss points with weight $w_i = 1/4$, the lumped mass matrix is obtained:

point 1:
$$\xi_i = 1$$
, $\eta_i = 0$, $\zeta_i = 0$, point 2: $\xi_i = 0$, $\eta_i = 1$, $\zeta_i = 0$
point 3: $\xi_i = 0$, $\eta_i = 0$, $\zeta_i = 1$, point 4: $\xi_i = 0$, $\eta_i = 0$, $\zeta_i = 0$

Here, the general formulation of mass matrix with a variable Gaussian integration point t is written as follows:

point 1:
$$\xi_i = t$$
, $\eta_i = \frac{1-t}{3}$, $\zeta_i = \frac{1-t}{3}$, (13)

point 2:
$$\xi_i = \frac{1-t}{3}$$
, $\eta_i = t$, $\zeta_i = \frac{1-t}{3}$
point 3: $\xi_i = \frac{1-t}{3}$, $\eta_i = \frac{1-t}{3}$, $\zeta_i = t$
point 4: $\xi_i = \frac{1-t}{3}$, $\eta_i = \frac{1-t}{3}$, $\zeta_i = \frac{1-t}{3}$

In Eq. (11), weight $w_i = 1/4$ so that $\sum_{i=1}^4 w_i = 1$, and $t \in [0,1]$. Using these four sampling points, the mass matrix can be formulated as:

$$\mathbf{M}^{e} = \frac{1}{4}V^{e} \begin{bmatrix} b_{11} & 0 & 0 & b_{14} & 0 & 0 & b_{17} & 0 & 0 & b_{110} & 0 & 0 \\ 0 & b_{22} & 0 & 0 & b_{25} & 0 & 0 & b_{28} & 0 & 0 & b_{211} & 0 \\ 0 & 0 & b_{33} & 0 & 0 & b_{36} & 0 & 0 & b_{39} & 0 & 0 & b_{312} \\ b_{41} & 0 & 0 & b_{44} & 0 & 0 & b_{47} & 0 & 0 & b_{410} & 0 & 0 \\ 0 & b_{52} & 0 & 0 & b_{55} & 0 & 0 & b_{58} & 0 & 0 & b_{511} & 0 \\ 0 & 0 & b_{63} & 0 & 0 & b_{66} & 0 & 0 & b_{69} & 0 & 0 & b_{612} \\ b_{71} & 0 & 0 & b_{74} & 0 & 0 & b_{77} & 0 & 0 & b_{710} & 0 & 0 \\ 0 & b_{82} & 0 & 0 & b_{85} & 0 & 0 & b_{88} & 0 & 0 & b_{811} & 0 \\ 0 & 0 & b_{93} & 0 & 0 & b_{96} & 0 & 0 & b_{99} & 0 & 0 & b_{912} \\ b_{101} & 0 & 0 & b_{104} & 0 & 0 & b_{107} & 0 & 0 & b_{1010} & 0 & 0 \\ 0 & b_{112} & 0 & 0 & b_{115} & 0 & 0 & b_{118} & 0 & 0 & b_{1111} & 0 \\ 0 & 0 & b_{123} & 0 & 0 & b_{126} & 0 & 0 & b_{129} & 0 & 0 & b_{1212} \end{bmatrix}$$

where

$$b_{11} = b_{22} = b_{33} = b_{44} = b_{55} = b_{66} = b_{77} = b_{88} = b_{99} = b_{10} = b_{11} = b_{12} = t^2 + \frac{(1-t)^2}{3}$$

The remaining parameters in Eq. (14) equal to $2t \frac{(1-t)}{3} + \frac{2(1-t)^2}{9}$

The summation of all matrix elements of \mathbf{M}^{e} equals to the volume of the element regardless of value of t:

$$\sum_{i=1}^{144} \frac{1}{12} V^e \left[12 \left(t^2 + \frac{(1-t)^2}{3} \right) + 36 \left(2t \frac{(1-t)}{3} + \frac{2(1-t)^2}{9} \right) \right]$$

$$= V^e$$
total mass of the element
$$(15)$$

3. Numerical examples

In this section, some examples will be analysed to demonstrate the properties of the present method. The triangular elements in 2D and tetrahedral elements in 3D are used.

4.1 2D examples

The first 2D cantilever beam with length l=1m and width d=0.2m is studied, which is subjected to fixed boundary condition at left hand side as outlined in Fig. 5

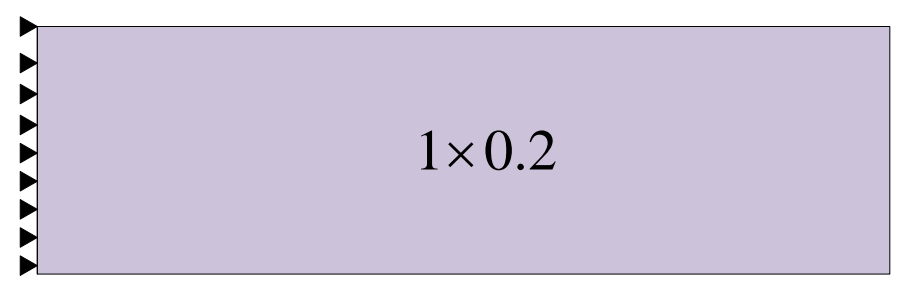


Figure 5: 2D cantilever beam

4.1.1 Effect of Gaussian integration point

As shown in Fig. 6, the effect of Gaussian integration point on the computation of eigenfrequency using FEM is presented. In order to show the applicability of the proposed method, mode shape 1 and 4 are studied. It is easily observed that the Gaussian integration point controls the value of eigenfrequency.

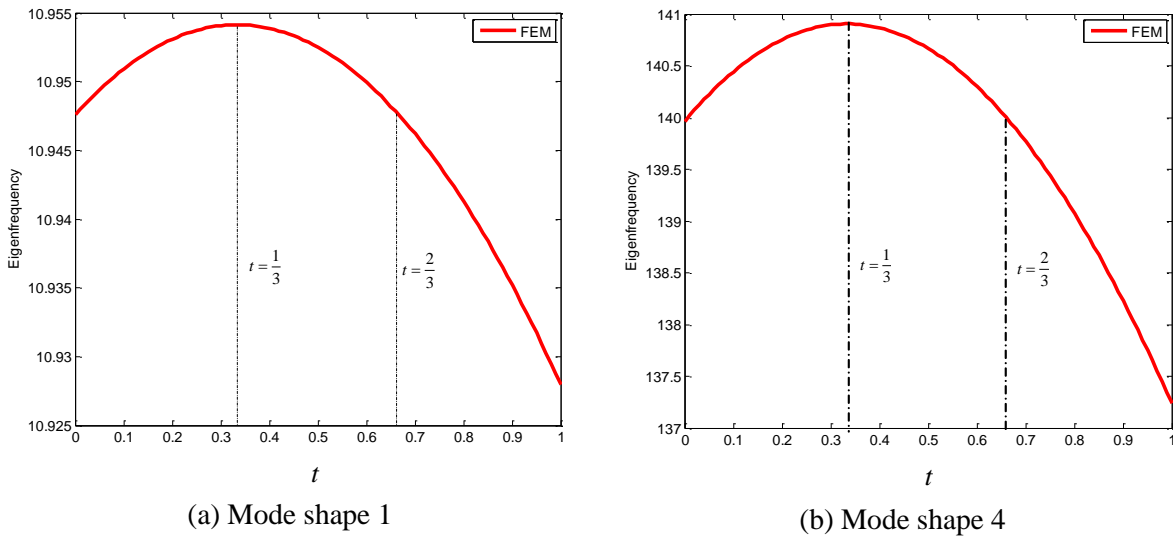


Figure 6: Effect of Gaussian integration point on eigenfrequency using FEM

As shown in Fig. 6, it is seen that t=1/3 provides the maximum eigenfrequency. As t=1 is corresponding to lumped mass matrix, the minimum eigenfrequency is obtained. While the eigenfrequency from t=2/3 which gives consistent mass matrix is less than value for t=1/3, but greater than the one using lumped mass matrix.

The convergence rate of eigenfrequency for mode shape 7 and 20 using different Gaussian integration point is presented in Fig. 7. It is clearly indicated that FEM with lumped mass matrix gives the most accurate results compared with consistent mass matrix. In addition, it is noticed that Gaussian integration t=1/3 always gives the maximum eigenfrequency.

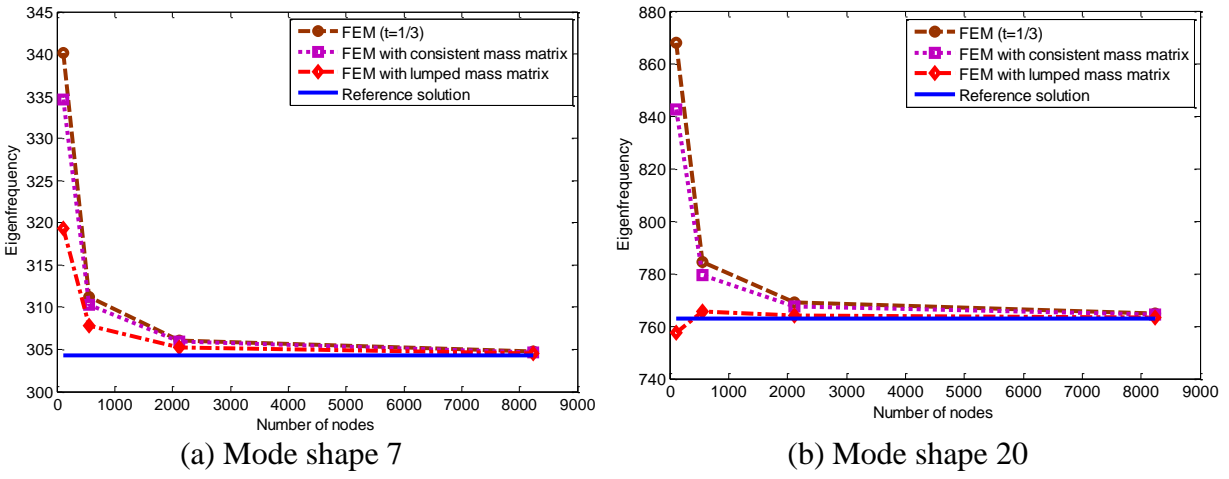


Figure 7: Convergence rate for different Gaussian integration point using FEM

4.2 3D examples

In this section, the mass-redistributed method is further extended to 3D problem.

4.2.1 Effect of Gaussian integration point

As shown in Fig. 8, a three dimensional cantilever beam with dimension $1\times0.2\times0.2$ m subjected to fixed boundary condition is studied. The eigenfrequency is computed to analyze the performance of mass-redistributed method.

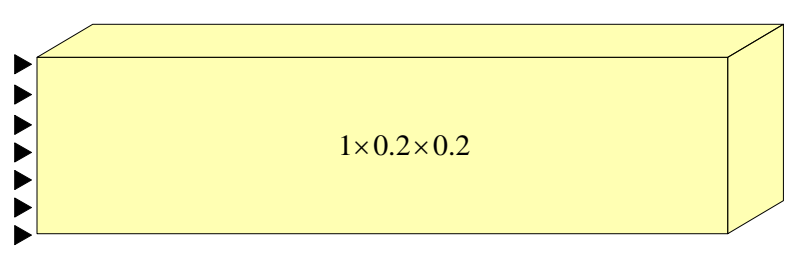


Figure 8: 3D cantilever beam

As outlined in Fig. 9, it is seen that the consistent mass matrix is corresponding to t=0.585. The minimum eigenfrequency is obtained as t equals to 1 (t=1 formulates the lumped mass matrix). It is seen that t=1/4 always provides the largest eigenfrequency as presented in Fig.9.

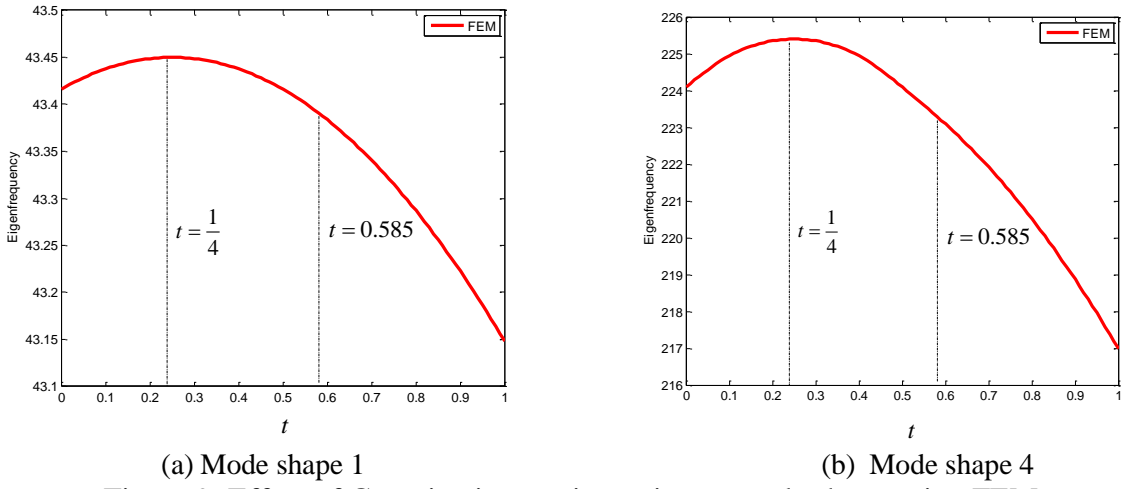


Figure 9: Effect of Gaussian integration point on mode shape using FEM

To further investigate the effect of mass-redistributed method in the evaluation of eigenfrequency, the convergence rate for mode shape 5 and 20 using different Gaussian integration point is shown in Fig. 10. Again, it is found that the lumped mass matrix always predicts much better solution compared with consistent mass matrix. The Gaussian integration point t=1/4 gives the largest solution of eigenfrequency. The solution from consistent mass matrix is always between the Gaussian integration point t=1 (corresponding to lumped mass matrix) and t=1/4.

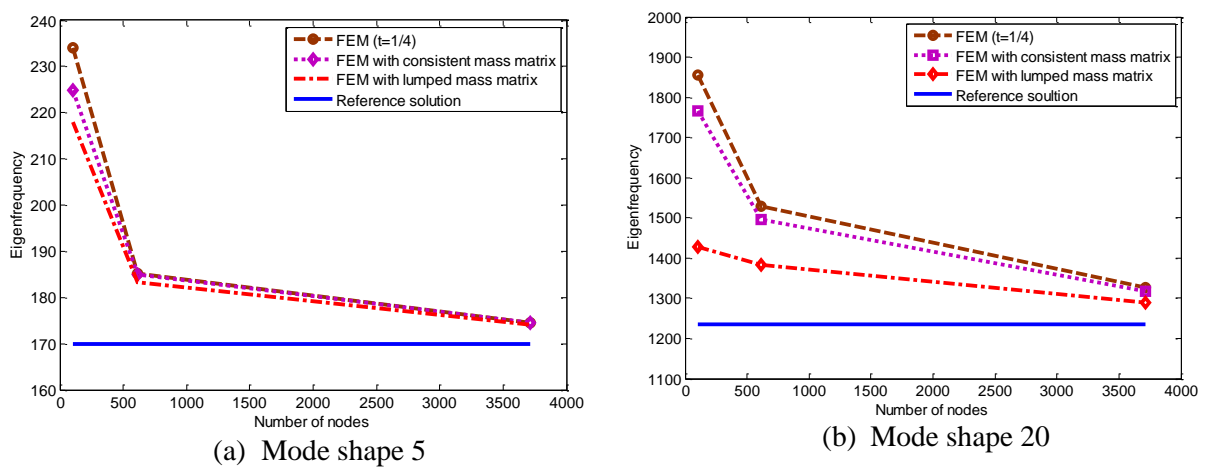


Figure 10: Convergence rate for different Gaussian integration point using FEM

4. Conclusion

In this paper, a mass-redistributed method is further developed for solving eigenfrerquency by modification of Gaussian integration point in the computation of mass matrix. In the present mass-redistributed method, the alternation of Gaussian integration point always ensures the mass conservation. The triangular and tetrahedral elements are focused in this study. Both theoretical and numerical results have demonstrated that the Gaussian integration point in the mass matrix has a significant effect on the prediction of eigenfrequency, and the following conclusions can be summarized:

- a) With adjustment of Gaussian integration point, the eigenfrequency of systems can be modified.
- b) The t=1/3 gives the maximum eigenfrequency in the 2D model; while t=1/4 results in the maximum eigenfrequency of 3D model
- c) Due to the correct balance between the stiffness and mass matrix, the lumped mass matrix has the best solution in the computation of eigenfrequency.

Acknowledgements

The project is supported by the Science Fund of State Key Laboratory of Advanced Design and Manufacturing for Vehicle Body Nos. 31315002 and 51375001. The authors wish to thank the National Natural Science Foundation of China (Grant No. 11202074) and Research Project of State Key Laboratory of Mechanical System and Vibration MSV201403for the support.

Reference

1. GR Liu. Meshfree methods: Moving Beyond the Finite Element Method, 2nd Edition, CRC Press:

- Boca Raton, USA, 2009.
- 2. GR Liu, TT Nguyen. Smoothed Finite Element Methods. Boca Raton: CRC Press; 2010.
- 3. GR Liu, T Nguyen-Thoi, KY Lam. An edge-based smoothed finite element method (ES-FEM) for static, free and forced vibration analyses in solids. Journal of Sound and Vibration, 320: 1100-1130, 2009.
- 4. Eric Li, G. R. Liu, Vincent Tan. Simulation of Hyperthermia Treatment Using the Edge-Based Smoothed Finite-Element Method. Numerical Heat Transfer, Part A: Applications. 2010; 57: 11, 822 -847
- 5. Z. C. He, G. Y. Li, Z. H. Zhong, A. G. Cheng, G. Y. Zhang, Eric Li, G. R. Liu. An ES-FEM for accurate analysis of 3D mid-frequency acoustics using tetrahedron mesh. Computers and Structures. 2012; 106-107: 125-134.
- 6. Z.C. He, A.G. Cheng, Z.H. Zhong, G.Y. Zhang, G.Y. Li, Eric Li. An improved eigenfrequencies prediction for three-dimensional problems using face-based smoothed finite element method. Journal of ActaMechanicaSolidaSinica. 2013; 26:140-150.
- 7. Z. C. He, G. Y. Li, Z. H. Zhong, A. G. Cheng, G. Y. Zhang, G. R. Liu, Eric Li, Z. Zhou. An edge-based smoothed tetrahedron finite element method (ES-T-FEM) for 3D static and dynamic problems. Computational mechanics. 2013; 2:221 -236.
- 8. Eric Li, Z.C. He, Xu Xu. A novel edge-based smoothed tetrahedron finite element method (ES-T-FEM) for thermomechanical problems. International Journal of Heat and Mass Transfer 66 (2013) 723–732.
- 9. Z. C. He, G. Y. Li, Eric Li, Z. H. Zhong, G. R. Liu. Mid-frequency acoustics analysis using edge-based smoothed tetrahedron radial point interpolation method (ES-T-RPIM). Computational methods DOI: 10.1142/S021987621350103X.
- 10. GR Liu, TNguyen-Thoi, H Nguyen-Xuan, KY Lam. A node-based smoothed finite element method (NS-FEM) for upper bound solution to solid mechanics problems. Computers and Structures, 87: 14-26, 2009.
- 11. GR Liu, T Nguyen-Thoi, KY Lam. A novel Alpha Finite Element Method (αFEM) for exact solution to mechanics problems using triangular and tetrahedral elements. Computer Methods in Applied Mechanics and Engineering, 197: 3883-3897, 2008.
- 12. Eric Li, G. R. Liu, Vincent Tan, and Z. C. He. Modeling and simulation of bioheat transfer in the human eye using the 3D alpha finite element method (αFEM). Intentional Journal for Numerical Methods in Biomedical Engineering. 2010; 26:955–976
- 13. Eric Li, G.R. Liu, Vincent Tan, Z.C. He. An efficient algorithm for phase change problem in tumor treatment using αFEM. International Journal of Thermal Sciences. 2010; 49: 10, 1954-1967.
- 14. Eric Li, ZP Zhang, ZC He, Xu Xu, GR Liu, Q Li. Smoothed finite element method with exact solutions in heat transfer problems. International Journal of Heat and Mass Transfer 78(2014) 1219-1231.
- 15. Eric Li, ZC He, L Chen, Xu Xu, GR Liu. An ultra-accurate hybrid smoothed finite element method for Piezoelectric problem. Engineering Analysis with boundary element 50 (2015) 188–197.
- 16. Eric Li, Xu Xu, Z. C. He, G.R. Liu. Hybrid smoothed finite element method for acoustic problems. Computer Methods in Applied Mechanics and Engineering 283 (2015) 664–688.
- 17. Eric Li, Zhongpu Zhang, CC Chang, GR Liu, Q Li. Numerical homogenization for incompressible materials using selective smoothed finite element method. Composites Structures 123 (2015) 216–232.
- 18. Marfurt KJ, Accuracy of finite difference and finite element modeling of the scalar and elastic wave equation, Geophysics.1984; 49: 533–549.
- 19. Murthy N, Guddati; Bin Yue. Modified integration rules for reducing dispersion error in finite element methods. Computer Methods in Applied Mechanics and Engineering 2004;193(3-5):275-287
- 20. ZC He, GY Li, GR Liu, AG Cheng, Eric Li. Numerical investigation of ES-FEM with various Mass re-distribution for acoustic problems. 89 (2015) 222–233